AD NUMBER: AD0467443

LIMITATION CHANGES

TO:

Approved for public release; distribution is unlimited.

FROM:

Distribution authorized to U.S. Gov't. agencies and their contractors; Administrative/Operational Use; 1 Nov 1964. Other requests shall be referred to Army Natick Labs, Natick, MA 01760

AUTHORITY

USANL LTR 4 DEC 1965

SECURITY MARKING

The classified or limited status of this report applies to each page, unless otherwise marked.
Separate page printouts MUST be marked accordingly.

THIS DOCUMENT CONTAINS INFORMATION AFFECTING THE NATIONAL DEFENSE OF THE UNITED STATES WITHIN THE MEANING OF THE ESPIONAGE LAWS, TITLE 18, U.S.C., SECTIONS 793 AND 794. THE TRANSMISSION OR THE REVELATION OF ITS CONTENTS IN ANY MANNER TO AN UNAUTHORIZED PERSON IS PROHIBITED BY LAW.

NOTICE: When government or other drawings, specifications or other data are used for any purpose other than in connection with a definitely related government procurement operation, the U. S. Government thereby incurs no responsibility, nor any obligation whatsoever; and the fact that the Government may have formulated, furnished, or in any way supplied the said drawings, specifications, or other data is not to be regarded by implication or otherwise as in any manner licensing the holder or any other person or corporation, or conveying any rights or permission to manufacture, use or sell any patented invention that may in any way be related thereto.

UTAH RESEARCH & DEVELOPMENT CO., INC.

SALT LAKE CITY, UTAH

Subsidiary of Interstate Engineering Corporation, Anaheim, California

SPONSORED BY:

Advanced Research Projects Agency
U. S. Army Natick Laboratories
Natick, Massachusetts
ARPA Order No. 267, Amendment No. 9

THEORETICAL AND EXPERIMENTAL STUDY OF LOW-VELOCITY PENETRATION PHENOMENA

SEMIANNUAL REPORT
Phases III, IV and V

November 1964

Contract DA-19-129-AMC-150(X)

Utah Research & Development Co.
1820 South Industrial Road
Salt Lake City, Utah 84104

Phone: 486-1301
TWX: 801-521-2680

TABLE OF CONTENTS

SUMMARY

The tensor formulation of the stress-strain relationships involved in finite time-dependent deformation of a solid has been changed from that previously reported. The new mathematical model is described along with a discussion of the applicable mathematics.

The computer code developed to calculate the flow field in impact has been modified to eliminate propagated error in the time dimension.

A system for high speed photographic analysis of deformation of wires and rods is described. Data from rod-to-rod impact are analyzed to determine the energies involved in metal deformation. Average energy per unit deformation is found to decrease with increasing impact velocity.

1. INTRODUCTION

The theoretical work described here is a continuation of work reported in June 1964 in "Final Report, Phases I and II, Theoretical and Experimental Study of Low Velocity Penetration Phenomena," Contract No. DA 19-129-AMC-150(X) (OI9114). The mathematical model for describing the force and flow field for a solid deforming under impact has been extensively revised. The new model is described in this report in Sections 2 and 3. The description is self contained although reference to the previous report may be necessary to follow the progress of the work. The earlier discussion of tensor notation and computational methods is equally applicable to this report. The possibility of rewriting the mathematics using differential notation rather than tensors was carefully considered but was rejected for the present because of lack of time and the advantages of the tensor notation for the general impact problem.

The computer codes used previously have been refined to avoid propagation of errors in the time domain. This is discussed in Section 4. Considerable work remains to modify the computer program to utilize the new mathematical model. This will be the major computational work of the next report period.

The experimental program to measure material properties by observing the deformation of a thin wire or rod during impact is progressing. The gun range and high-speed photographic equipment are operating and various techniques have been developed for observing and measuring deformation. This work is described in Section 6.

Data available from other work, involving the impact of rods on rods, has been analyzed to determine the relations among energy, deformation, and impact velocity. The results are presented in Section 7. This work will continue next quarter and transient deformation will be observed with the high-speed photographic equipment. The geometry of the deformation will be observed as a test of the computer program.

2. CONTINUUM THEORY OF DEFORMATION MECHANICS

2.1 Coordinates

In describing deformation, we shall use three sets of coordinates, i.e. underlying, initial, and deformed (or material).

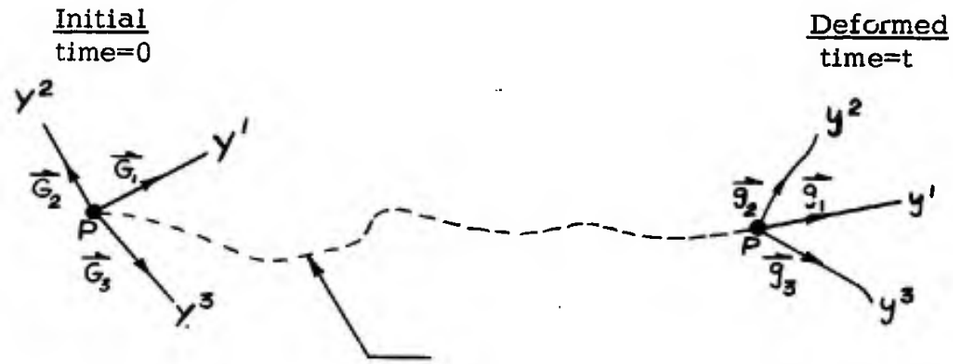

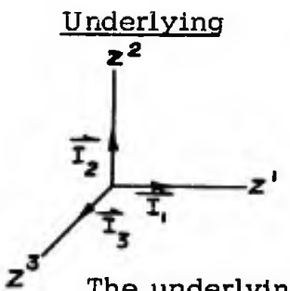

The underlying coordinates z^i are orthonormal with orthonormal vector basis $\vec{I}_i$. These coordinates provide the ultimate reference for defining other coordinates.

The initial coordinates are defined in terms of the underlying coordinates at time=0. Throughout the region that is initially occupied with matter, we give each mass point a label which remains with it at all later times. This label is simply the initial coordinates of the mass point. This essentially "imbeds" a copy of the initial coordinates in the material.

As time passes, the material moves and deforms and the mass points have new spatial positions. The initial coordinates are still unchanged, but the "copy" that was imbeded in the material has been carried along and deformed with the material. This deformed copy of the initial coordinates is called the deformed or material (because it is imbedded in the material) coordinates.

The initial coordinates are usually (but not necessarily) the coordinates used to describe the spatial positions of the mass points as they move. Therefore, the initial coordinates are also the spatial coordinates.

The deformation is described by giving the spatial coordinates of each mass point as functions of time. Symbolically, this mapping can be written

$$Y^i = F^i \circ (y^j, t)$$

or conversely $$y^i = f^i \circ (Y^j, t)$$

A material point P, is considered to retain its identity wherever it is described. The label of material point P, is y^i; its spatial coordinates are Y^i.

$$\text{mass point} \equiv P \equiv P(y^i)$$

$$\text{has coordinates} \quad Y^j \circ (y^i)$$

Note that at time zero, point P has coordinates

$$Y^j = y^j$$

Later the coordinates Y^i may be some general functions of y^j and time.

The y^i are often called the Lagrangian coordinates and the y^i the Eulerian coordinates (26:64), (1:6).* The ordered triple y^i is the "label" of a material point, and Y^i gives its spatial position.

The initial coordinates are defined in terms of the underlying coordinates by some relations H^i

$$Y^i = H^i \circ (z^j)$$

or inversely $$z^i = h^i \circ (Y^j)$$

We define the local, tangent vector basis in the Y^i coordinates by (1:7)

---

* Numbers in parentheses refer to references in Section 5. The number preceding the colon is the reference number and the number following the colon is the page number.

$$\hat{\vec{G}}_i = \frac{dz^j}{dY^i}\,\hat{\vec{I}}_j = \frac{dh^j}{dy^i}\,\hat{\vec{I}}_j = A_i{}^j\hat{\vec{I}}_j$$

For convenience in writing, we define $A_i{}^j = \frac{dh^j}{dy^i}$

The functions H^i and F^i are assumed to be well behaved with the usual qualifications. See Eringen (1:6).

The local metric at Y^i is the array of dot products of the local basis vectors. G_{ij} is a function of Y^i.

$$G_{ij} = \hat{\vec{G}}_i \cdot \hat{\vec{G}}_j$$

$$= A_i{}^m A_j{}^n \hat{\vec{I}}_m \cdot \hat{\vec{I}}_n = A_i{}^m A_j{}^n \,\delta_{mn}$$

$$G_{ij} = A_i{}^m A_j{}^m$$

The local vector basis in the material coordinates is

$$\hat{\vec{g}}_i = \frac{dY^j}{dy^i}\,\hat{\vec{G}}_j$$

$$\hat{\vec{g}}_i = B_i{}^j \hat{\vec{G}}_j$$

where $$B_i{}^j = \frac{dY^j}{dy^i}$$

The metric as a function of y^i is

$$g_{ij} = B_i{}^m B_j{}^m$$

The metric tensor is $$\underset{2}{g} = g_{ij}\, g^i \otimes g^j$$

2.2 Strain

When a material is deformed stresses arise in it, or conversely, deformation results when stresses are applied to a deformable body. We must first of all have coordinate invariant ways to describe stress and strain and then postulate relations between them.

Take a material point at time zero and consider any arbitrary infinitesimal vector $\hat{\vec{dR}}$ emanating from it.

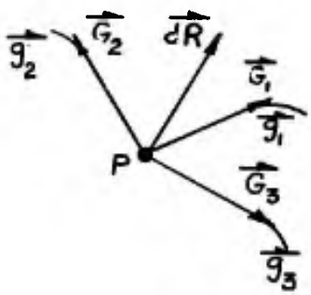

time=0

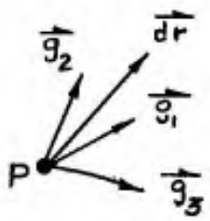

time = t

At time zero

$$\vec{G}_i = \vec{g}_i$$

$$Y^i = y^i$$

So that initially $\quad d\vec{R} = dY^i \vec{G}_i = dy^i \vec{g}_i$

and $\quad d\vec{R} = dy^i \vec{G}_i = dY^i \vec{g}_i$

At time t, $d\vec{R}$ has been deformed, or mapped, into $d\vec{r}$.

$$d\vec{r} = y^i \vec{g}_i$$

The squares of the lengths of $d\vec{R}$ and the corresponding $d\vec{r}$ are

$$dS^2 = d\vec{R} \cdot d\vec{R}$$

$$dS^2 = dy^i\, dy^j\, \vec{G} \cdot \vec{G}_j$$

$$dS^2 = G_{ij}\, dy^i\, dy^j$$

$$ds^2 = d\vec{r} \cdot d\vec{r}$$

$$ds^2 = dy^i\, dy^j \vec{g}_i \cdot \vec{g}_j$$

$$ds^2 = g_{ij}\, dy^i\, dy^j$$

These lengths are in terms of the imbedded or material coordinates. In other words, we follow an infinitesimal vector imbedded in the material at a given material point $P(y^i)$, and see how its length changes. It is useful to compare its original length at time zero to its length at time t. See Coburn (36:248).

$$ds^2 - dS^2 = (g_{ij} - G_{ij})\, dy^i\, dy^j$$

The material, or Lagrangian, strain tensor is defined as

$$e_{ij} = 1/2\ (g_{ij} - G_{ij})$$

This tensor is a function of the material coordinates y^k.

$$e_{ij} = 1/2 \left[g_{ij}(y^K) - G_{ij}(y^K) \right]$$

G_{ij} was defined as a function of the initial coordinates Y^K.

$$G_{ij}(Y^K) = A_i{}^m(Y^K)\ A_i{}^m(Y^K)$$

Since the appearance of G_{ij} in the strain formula is for time zero, when $y^i = Y^i$ numerically, we just replace Y^i by y^i in calculating G_{ij}.

$$e_{ij} = 1/2 \left[B_i{}^m B_j{}^m - G_{ij} \right]$$

where $B_i{}^m$ is the transformation of $\vec{G}_i$ to $\vec{g}_i$.

The strain tensor is a second order tensor which may be referred to a second order tensor basis. For example:

$$\underset{\sim}{e}^{2} = e_{ij}\ \hat{g}^i \otimes \hat{g}^j = e_{ij}\ \underset{\sim}{g}^{2}\ ij$$

or

$$\underset{\sim}{e}^{2} = e^{ij}\ \underset{\sim}{g}^{2}_{ij} = e^i{}_j\ \underset{\sim}{g}^{2}_i\ {}_j = e_i{}^j\ \underset{\sim}{g}^{2}_j\ i$$

The tensor itself $\underset{\sim}{e}^{2}$, should not be confused with its component representation e_{ij} with respect to the tensor basis $\hat{g}^i \otimes \hat{g}^j \equiv \underset{\sim}{g}^{2}\ ij$.

The difference in deformed arc length to initial arc length is now

$$dS^2 - ds^2 = 2\ e_{ij}\ \underset{\sim}{g}^{2}\ ij \odot (\vec{dP} \otimes \vec{dP})$$

where $\vec{dP} = dy^i \hat{g}_i$ and the dot in the circle stands for the contraction of the tensor product

$$dS^2 - ds^2 = 2\ e_{ij}\ dy^i\ dy^j\ \underset{\sim}{g}^{2}\ ij \odot \underset{\sim}{g}^{2}_{ij}$$

$$dS^2 - ds^2 = 2\ e_{ij}\ dy^i\ dy^j$$

The covariant e_{ij} and contravariant forms of the strain tensor are clearly symmetric. The mixed forms generally are not.

$$e_i^{\ j} = e_{ik}\, g^{kj}$$

where g^{kj} is the inverse of g_{kj} so that

$$g^{ik}\, g_{kj} = \delta^i_{\ j}$$

Substituting our definition of strain for e_{ik} we get

$$e_i^{\ j} = 1/2\ (g_{ik} - G_{ik})\ g^{kj}$$

$$e_i^{\ j} = 1/2\ (\delta_i^{\ j} - G_{ik}\, g^{ky})$$

This expression needs some physical interpretation.

Because $B_i^{\ j}$ is readily available in our discrete variable scheme (to be explained later), the above strain formulation is more convenient than the conventional (1:15)(26:69) one below:

$$2E_{KL} = \frac{dU^K}{dY^L} + \frac{dU^L}{dY^K} + \frac{dU^M}{dY^K}\ \frac{dU^M}{dY^L}$$

where for simplicity of notation, U^K_L are the displacement vector components referred to cartisian coordinates Y^L.

Most workers use the stress tensor to describe the stresses in a material. They then postulate some tensor relation between the stress and strain tensors that describes the physical properties of the material. There is much disagreement about any but the simplest (e.g. Hooke's law) tensor stress-strain relations. We have at our disposal a convenient means of calculating the strain tensor and hence the corresponding stress tensor, when the tensor stress-strain rule is given.

2.3 Stress

The state of stress at any material point can be completely described by the stress tensor.

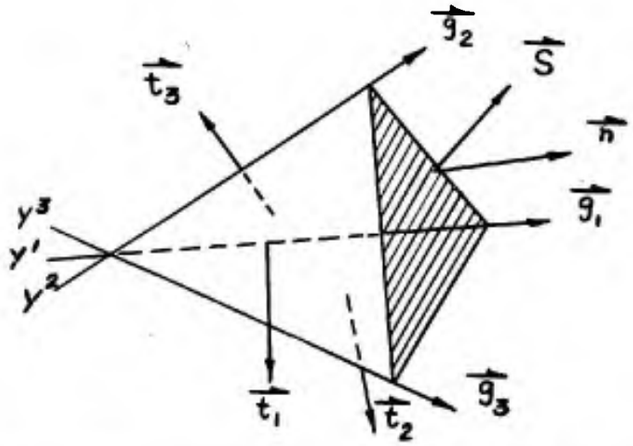

$\vec{T}^i = T^{ik}\,\vec{g}_k$ is the stress vector across the i-th coordinate surface.

$\vec{g}_i$ is the local basis

y_i are the coordinates

$\vec{n} = n^k\vec{g}_k$ is the unit normal to the shaded face

$\vec{S} = S^k\vec{g}_k$ is the stress vector across the shaded face

ρ is density of material in figure

Δv is volume of the figure

ΔA^i are areas of sides on coordinate surfaces

Δa is the area of shaded face

$\vec{V}$ is the velocity vector inside the figure

Newton's Law

$$\frac{d}{dt}(\rho \Delta v \vec{V}) = \vec{S}\,\Delta a - \vec{T}^i \Delta A^i$$

$$\frac{d}{dt}\left(\rho \frac{\Delta v}{\Delta a} v\right) = \vec{S} = \vec{T}^i \frac{A^i}{a}$$

$$\lim \frac{\Delta V}{\Delta a} = 0$$

so that

$$0 = \vec{S} - \vec{T}^i \frac{\Delta A^i}{\Delta a}$$

$$\vec{S}\,\Delta a = \vec{T}^i\,\Delta A^i$$

The four faces of the figure form a closed surface so that by using a vector theorem (39:250, 198, 144)

$$\vec{\Delta a} = \sum_i \frac{\Delta A_i}{\sqrt{g^{\underline{ii}}}} \vec{g}^i$$

where $\vec{\Delta a} = \vec{n}\, \Delta a$

so that $\vec{n} = \frac{\Delta A_i}{\Delta a} \vec{g}^i \sqrt{g^{\underline{ii}}}$

so that $\sqrt{g^{\underline{ii}}}\, n_i = \frac{\Delta A_i}{\Delta a}$

substituting into $\vec{S} = \vec{t}_i \frac{\Delta A_i}{\Delta a}$

we get $\vec{S} = \vec{T}^i\, n_i\, \sqrt{g^{\underline{ii}}}$

$$\vec{S} = T^{ij} \vec{g}_j\, n_i \sqrt{g^{\underline{ii}}}$$

$$S^j \vec{g}_j = n_i\, T^{ij}\, g_j \sqrt{g^{\underline{ii}}}$$

We define the stress tensor $\overset{2}{\vec{t}}$ as (39:251)

$$\overset{2}{\vec{t}} = t^{ij}\, \overset{2}{\vec{g}}_{ij} = \sqrt{g^{\underline{ii}}}\; T^{ij}\, \overset{2}{\vec{g}}_{ij}$$

or in component form

$$t^{ij} = \sqrt{g^{\underline{ii}}}\, T^{ij}$$

inversely $T^{ij} = \frac{t^{ij}}{\sqrt{g^{\underline{ii}}}}$

The stress vector $\vec{S}$ is contravariant and is given in terms of the stress tensor by

$$S^j \vec{g}_j = n_i\, t^{ij}\, \vec{g}_j$$

2.4 Hooke's Law in Tensor Form

Eringen shows the general requirements for stress-strain rules (1:135-140). One of the most fundamental is that the stress-strain relation must not depend on the orientation of the spatial coordinates. With this in

mind, we shall try to decide what measures of deformation the stress tensor may properly depend on. To be independent of the coordinates, the functional dependence must be a tensor equation and therefore all the quantities appearing in it must be tensors.

Deformation is measured relatively, i.e. by comparing the material at time t, to the material at time zero.

As a starting point, let us take the isotropic Hooke's law (1:160) in component form

$$t_i^{\ j} = \lambda e_k^{\ k} \delta_i^{\ j} + 2\mu e_i^{\ j}$$

This result is obtained by Eringen (1:154-160) from much more complicated general theory.

Presumably in an elastic material there is a relation between the stress and strain tensors as follows (3:59)

$$t_i^{\ j} = f_i^{\ j} \cdot (e_m^{\ k})$$

where $t_i^{\ j} \equiv 0$ when $e_m^{\ k} \equiv 0$ so that there are no initial stresses in the material.

Generalized, Hooke's law can be motivated by considering a power series expansion of the functionals $f_i^{\ j}$ in $e_i^{\ j}$ (3:58-59).

$$t_i^{\ j} = f_i^{\ j} \cdot (e_m^{\ k}) = C_{i\,k}^{\ j\ m} + \overline{C1}_{i\,k}^{\ j\ m} e_m^{\ k} + \overline{C2}_{i\,k}^{\ j\ m} e_m^{\ n} e_n^{\ k} + \overline{C3}_{i\,k}^{\ j\ m} e_m^{\ n} e_n^{\ r} e_r^{\ k} + \ldots .$$

Note that a power of a tensor is a tensor of the same order. For example,

$$\underset{2}{e} = e_i^{\ j}\, \underset{1}{g}^i \otimes g_j = e_i^{\ j}\, \underset{2}{g}\, i_j$$

$$\underset{2}{e}^{[2]} = \underset{2}{e} \odot \underset{2}{e} = e_i^{\ k} e_k^{\ m}\, \underset{2}{g}\, i_j$$

$$\underset{2}{e}^{[3]} = \underset{2}{e} \odot \underset{2}{e} \odot \underset{2}{e}$$

. . . . . etc.

The C's are constants which may depend on the coordinates and orientation, but not on $\overset{2}{e}$. The first term C, is just a constant term and is dropped because we assumed that $t_i^{\ j} = 0$ when $e_i^{\ j} = 0$.

Retaining only the linear second term in the power series (1:463) we have (26:83)(3:59)

$$t_i^{\ j} = \overline{Cl}_{i\ k}^{\ j\ m}\, e_m^{\ k}$$

For an isotropic material $\overline{Cl}$ must be (26:83-84) (3:65) an isotropic tensor which has the general form (26:44) (16:65-69)

$$\overline{Cl}_{i\ k}^{\ j\ m} = a\ \delta_i^{\ j}\ \delta_k^{\ m} + B\ \delta_i^{\ k}\ \delta_j^{\ m} + C\ \delta_i^{\ m}\ \delta_j^{\ k}$$

Then $$t_i^{\ j} = a\ \delta_i^{\ j}\ e_k^{\ k} + B\ e_j^{\ i} + C\ e_i^{\ j}$$

Because $e_{ij} = e_{ji}$ it can be shown that there are only two independent constants

$$t_i^{\ j} = a\ \delta_i^{\ j}\ e_k^{\ k} + D\ e_i^{\ j}$$

The scalars a and D are zero order tensors. They must be independent of coordinate descriptions. They may be any analytic functions of any scalar invariants.

2.5 Discussion of Coordinate Invariance

Coordinate invariance of stress-strain relations should be clarified. Perhaps the simplest way would be to give an example.

It is crucial to keep the various coordinate systems distinct and well defined. To simplify this problem, we will show the drawings in only two dimensions. The generalization is trivial.

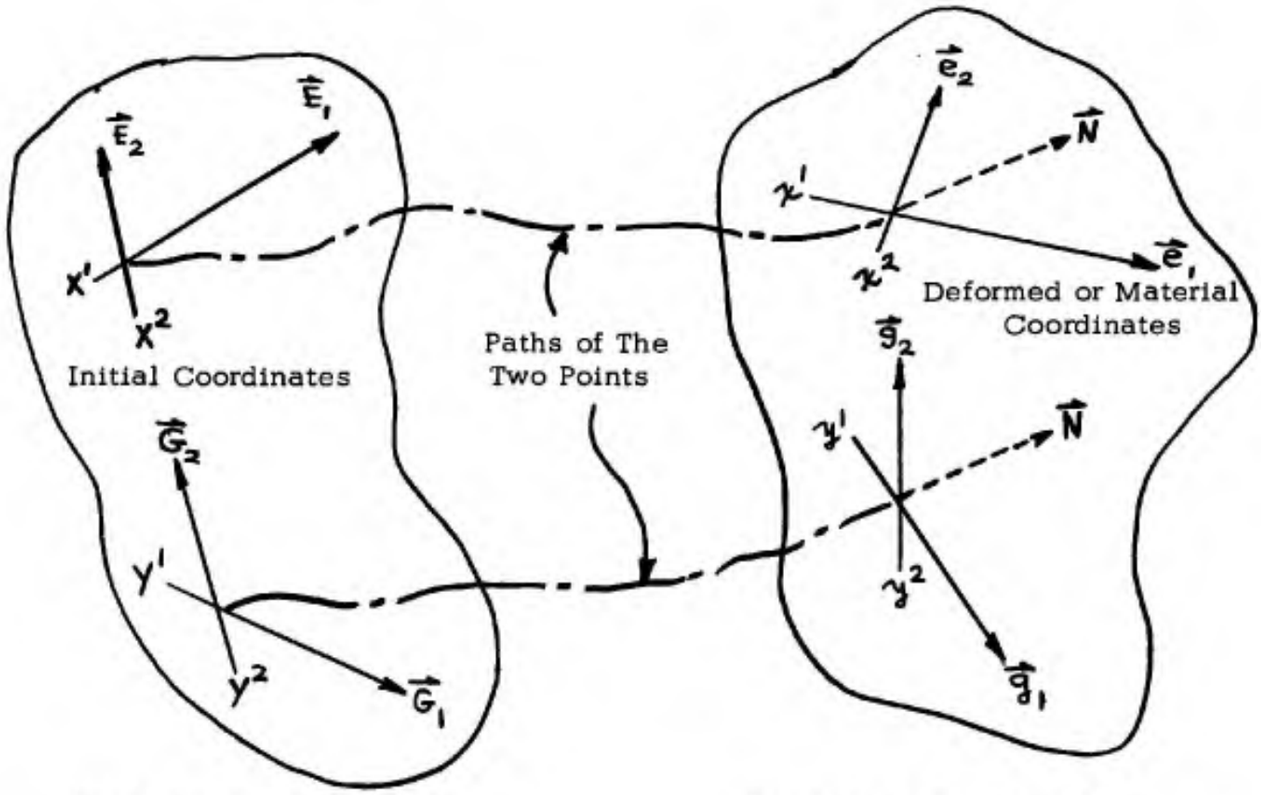

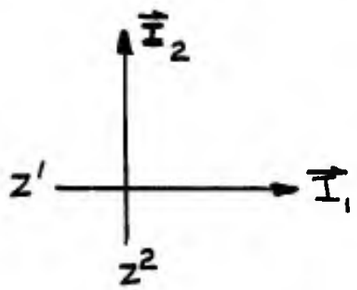

Underlying Coordinates

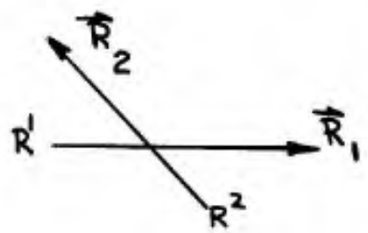

General Spatial Coordinates

In examination of the drawing, the following points should be noted:

1. Everything is ultimately referred to the underlying orthonormal cartesian coordinates Z^i with associated vector basis $\vec{I}_i$.

2. The deformation is observed in the general spatial coordinates R^i with associated local vector basis $\vec{R}_i$.

3. Two independent coordinate systems X^i and Y^i are chosen arbitrarily at time zero. Copies of these are imbedded in the material so as to move and deform with it. The initial coordinates X^i and Y^i have respective local vector bases $\vec{E}_i$ and $\vec{G}_i$.

4. The copies of the initial coordinates which are imbedded in the material are transformed with time to become the deformed or material coordinates. These are y^i and x^i with corresponding local vector bases $\vec{g}_i$ and $\vec{e}_i$, respectively.

5. The encircled region (local region at time zero) containing the two initial coordinate systems is chosen to be infinitesimal, so that the corresponding region after a well behaved transformation is also infinitesimal. This implies that these regions have linear geometry, i.e. are completely described by any of their various local vector bases.

6. The vector $\vec{N}$ (appearing twice in the deformed region), is the normal to some arbitrary plane cutting through the region. This is a plane across which we wish to find the stress vector.

The initial coordinate systems Y^i and X^i are transformed to the deformed coordinates y^i and x^i. If we calculate the strain tensors in the y^i and x^i references, the result should be different component representations of the same tensor. Now suppose that the stress-strain relation is some tensor equation such as

$$t_i^{\ j} = f \circ (e_i^{\ j})$$

There will be two forms of the stress tensor $t_i^{\ j}$, resulting from the two forms of the strain tensor. They should be the same stress tensor in different representations. The stress vector $\vec{S}$, across some arbitrary surface with normal N, is

$$\vec{S} = t_i^{\ j}\, n^i\, \vec{g}_j$$

in the y^i coordinates, and

$$\hat{\vec{S}} = t_i^{\ j}\, n^i\, \hat{\vec{e}}_j$$

in the x^i coordinates.

The components $t_i^{\ j}$ and n^i are of course relative to whatever coordinates in which the calculation is being made, i.e. the y^i or x^i coordinates. The two resulting stress vectors $\hat{\vec{S}}$, should be the same vector in different representations, because the two initial coordinate systems Y^i and X^i, have actually undergone the <u>same</u> deformation. The components of $\hat{\vec{S}}$ in the $\hat{\vec{e}}_i$ basis should be exactly equivalent to the components of $\hat{\vec{S}}$ in the $\hat{\vec{g}}_i$ basis. In fact, transforming the components of $\hat{\vec{S}}$ relative to the $\hat{\vec{g}}_i$ basis over the $\hat{\vec{e}}_i$ basis should yield the numerical equals of the components of $\hat{\vec{S}}$ <u>as calculated</u> in the $\hat{\vec{e}}_i$ basis. This is an example of the test of coordinate invariance.

The stress vector across a given plane resulting from a given strain must not change with (i.e. be dependent on) the coordinate description.

Suppose that H gives the components of $\hat{\vec{E}}_i$ relative to $\hat{\vec{G}}_i$ and A is the transformation taking $G_i^{\ j}$ to g_i.

$$\hat{\vec{E}}_i = H_i^{\ j}\, \hat{\vec{G}}_j$$

$$\hat{\vec{g}}_i = A_i^{\ j}\, \hat{\vec{G}}_j$$

If copies of both $\hat{\vec{E}}_i$ and $\hat{\vec{G}}_i$ are imbedded in the material at time zero, the components of $\hat{\vec{g}}_i$ relative to $\hat{\vec{e}}_i$ will remain the same throughout the deformation.

$$\hat{\vec{e}}_i = H_i^{\ j}\, \hat{\vec{g}}_j$$

in other words,

$\hat{\vec{e}}_i$ are to $\hat{\vec{g}}_j$ as

$\hat{\vec{E}}_i$ are to $\hat{\vec{G}}_j$

which means they have undergone the same deformation

$$\hat{\vec{g}}_j = h_j^{\ i}\, \hat{\vec{e}}_i$$

$$\hat{\vec{G}}_j = h_j^{\ i}\, \hat{\vec{E}}_i$$

where $h_j^{\ i}$ is inverse of $H_j^{\ i}$

Substituting into $\vec{g}_i = A_i^{\ j}\, \vec{G}_j$ we get

$$h_i^{\ n}\, \vec{e}_n = A_i^{\ k}\, h_k^{\ m}\, \vec{E}_m$$

multiplying both sides by $H_j^{\ i}$

$$\vec{e}_j = H_j^{\ i}\, A_i^{\ k}\, h_k^{\ m}\, \vec{E}_m$$

2.6 Rate of Deformation

In many materials the rate of deformation seems to influence the stresses. Therefore, we should find a tensor to measure this rate. The obvious starting place is the time derivative $\dot{e}_{ij}$, of the strain tensor.

$$\dot{e}_{ij} = \frac{d}{dt}\, e_{ij}$$

These quantities can easily be shown to be the components of a tensor.

The strain rate deviator is probably a better descriptor. The strain deviator is

$$D_i^{\ j} = e_i^{\ j} - \frac{1}{3}\, e_k^{\ k}\, g_i^{\ j}$$

$$D_{ij} = e_{ij} - \frac{1}{3}\, e_k^{\ k}\, g_{ij}$$

The strain rate deviator is

$$\dot{D}_i^{\ j} = \frac{d}{dt}\, D_i^{\ j}$$

2.7 More General Stress-Strain Rules

Stress and strain can be expressed as functions of the parameter time. During an infinitesimal time interval Δt, there will occur corresponding infinitesimal changes in stress and strain, Δe_{ij} and Δt_{ij}, respectively.

A rather general assumption for isotropic materials is that the change in stress is related to the change in strain

$$\Delta t_{ij} = f_{ij} \bullet (\Delta e_{ke})$$

Suppose we specialize this somewhat by using extended Hooke's law.

$$\Delta t_i^{\ j} = A\, \sigma_i^{\ j}\, \Delta e_k^{\ k} + B\, \Delta e_i^{\ j}$$

Dividing by Δt and passing the limit we get

$$\frac{dt_i^{\ j}}{dt} = A\, \sigma_i^{\ j}\, \frac{d}{dt}\, e_k^{\ k} + B\, \frac{de_i^{\ j}}{dt}$$

The scalars A and B may be any zero order tensors. This gives this relation its power. We may use all sorts of stress and strain and rate invariants to build A and B. Certainly within any small enough interval, the stress-strain must be very close to linear. The constants A and B simply give the slope of the relation.

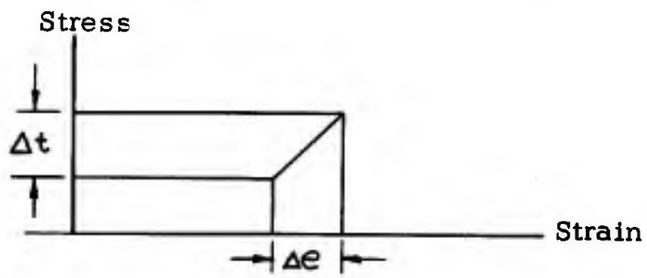

Schematically, the stress depends on the stress at the beginning of the interval and the slope.

We have not decided on the exact structure of the scalars A and B, but some of the invariants to be used were discussed in the last report.

By judiciously choosing the structure of A and B, many material effects can be expressed. For example: nonlinearity in the elastic range, plastic flow rate dependence, fracture level, plastic yield level, work hardening, heating, stored elastic energy while flowing plastically.

3. DISCRETE VARIABLE MODEL

3.1 Introduction

Due to the extreme complexity and nonlinearity of the continuum formulation, it was considered prudent to avoid attacking the problem with continuous variable methods. Great simplifications can be effected by transforming the continuum equations into discrete variable approximation. The question immediately arises: how good is the approximation? This very important inquiry is not easy to answer. As the development of the discrete variable model proceeds, we will try to give at least intuitive arguments to justify our approximations.

The problem is best described, for computational purposes, in a peculiar mixture of coordinate representations. The stress-strain relations are most easily evaluated in the material coordinates. However, the kinematical aspect of the situation is very complicated in the material coordinates because the metric is time dependent and, in general, quite arbitrary. Therefore, the stresses and strains are calculated in the material coordinates and the kinematics is conducted in the spatial coordinates. The mathematical connection between the two coordinate representations is used to transform the resultant force vector (as calculated in the material coordinates from the local values of the stress tensor) at a mass point to the spatial coordinates. The force vector then enters the relatively simple spatial kinematical relationship (i.e. Newton's Law).

3.2 Discrete Variable Mesh

The initial coordinates Y^i are defined in terms of the underlying orthonormal coordinates Z^i.

$$y^i = f \cdot (z^j)$$

$$z^i = F \cdot (y^j)$$

A copy of the Y^i is imbedded in the material at time zero. This copy deforms with the material to become the material coordinates.

In the region occupied by the material, lumped mass points are located at the intersections of the material coordinate lines which are ΔY^i apart. For convenience of representation, the illustrative figures are shown in two dimensions only.

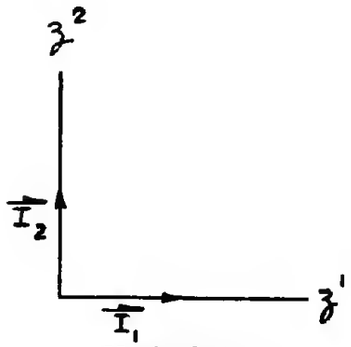

Underlying

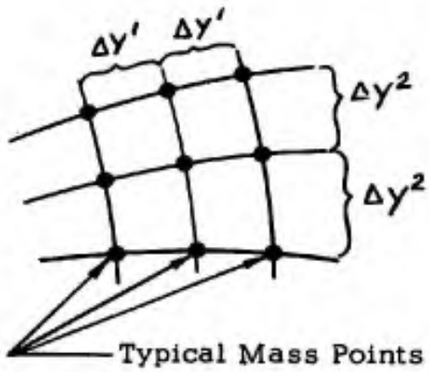

Initial

Note that since the numerical values of a mass point in the material coordinates are the same as its initial coordinates at time zero, $\Delta Y^i = \Delta y^i$ numerically, but not geometrically. The initial coordinates, once chosen, remain fixed during the deformation. In the discrete variable scheme, the material coordinates are defined by connecting the positions of the discrete mass points with straight lines. This is a reasonable approximation since the spacing between mass points is assumed to be small enough so that the material coordinate lines connecting the mass points can be considered almost straight (as viewed from the underlying coordinates).

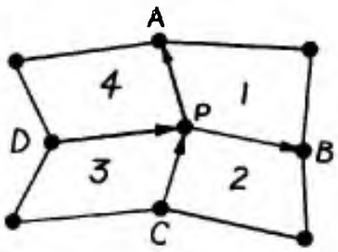

In order to calculate the strain tensor at a mass point, we must know the transformation connecting the local tangent vector basis in the spatial coordinates with the local basis in the material coordinates. For convenience, the underlying orthonormal coordinates will be used as the spatial coordinates. This will simplify the numerical calculations greatly. The positions and kinematics of the discrete mass points are reckoned in the underlying coordinates z^i. At the point P, there are four local tangent bases. The basis in

quadrant 1 is determined by vectors $\vec{PA}$ and $\vec{PB}$
quadrant 2 is determined by vectors $\vec{PB}$ and $\vec{PC}$
quadrant 3 is determined by vectors $\vec{PC}$ and $\vec{PD}$
quadrant 4 is determined by vectors $\vec{PD}$ and $\vec{PA}$.

In the discrete variable scheme, we tabulate the spatial position (in terms of the underlying coordinates) of each mass point as deformation progresses. This will furnish the connection between the material and spatial coordinates which is needed to calculate the metric of the material coordinates. The strain tensor is found from the initial and material metrics.

The connection can be expressed as the four linear transformations of the initial local basis $\hat{G}_i$, at material point P into the four deformed bases around point P at a later time. In terms of the underlying or spatial coordinates, the local basis in the material coordinates y^i is

$$\hat{g}_i = \frac{dz^j}{dy^i} \hat{I}_j$$

Let $U_i^{\ j} = \frac{dz^j}{dy^i}$ for ease of symbolism.

Then $$\hat{g}_i = U_i^{\ j} \hat{I}_j$$

The deformed metric is $$g_{ij} = U_i^{\ k} U_j^{\ k}$$

One can see that $U_i^{\ k}$ is just the array of the components of the $\hat{g}_i$ relative to the underlying basis $\hat{I}_i$. For example, to find the components of vector $\overrightarrow{PB}$ (see figure) we simply subtract the spatial coordinates $z^i(B)$ of point P from the spatial coordinates $z^i(P)$ of B, divided by ΔY^i

$$\overrightarrow{PB} = \overline{BP}^i \hat{I}_i$$

where $$\overline{PB}^i = \frac{z^i(B) - z^i(P)}{\Delta y^i}$$

In quadrant one of the figure, the transformation would be

$$\begin{bmatrix} U_1^{\ 1} & U_1^{\ 2} \\ U_2^{\ 1} & U_2^{\ 2} \end{bmatrix} = \begin{bmatrix} \overline{PB}_1 & \overline{PB}_2 \\ \overline{PA}_1 & \overline{PA}_2 \end{bmatrix}$$

The other quadrants are handled similarly.

To calculate the initial metric G_{ij}, the same procedure is used as above, but the positions of the mass points will be given by some analytic formula instead of being tabulated.

3.3 Strain Tensor

The four strain tensors around each mass point are given by

$$e_{ij} = 1/2 \left[g_{ij} - G_{ij} \right]$$

where $$g_{ij} = U_i^{\ k} U_j^{\ k}$$

3.4 Equation of Motion

In curvilinear coordinates, Newton's Law becomes (Coburn:253)

$$\frac{\nabla t^{ij}}{dy^i} = \rho a^i$$

where $\frac{\nabla}{dy^i}$ is the covariant differentiation operator

ρ is the density

a^i are the components of the acceleration vector

t^{ij} is the stress tensor

Our intention is to find the acceleration $\vec{a}$, that the local stress imbalance produces, and transform it to the spatial coordinates to make the kinematical calculations.

$$a^i = \frac{1}{\rho} \frac{\nabla t^{ij}}{dy^i}$$

To find a^i we must compute ρ and evaluate the derivative. Now approximations enter.

$$\frac{\rho_o}{\rho} = \frac{V}{V_o} \quad \text{or} \quad \rho = \rho_o \frac{V_o}{V}$$

where ρ_o and V_o are the initial values. The expression for ρ is rather clumsy, and the covariant derivative is much worse. Therefore, we shall propose a reasonable approximation which is more convenient computationally.

For the moment, let us consider just one quadrant around the material point P

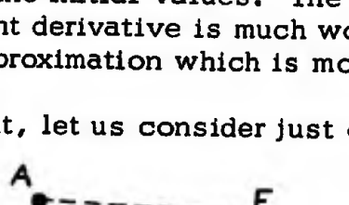

Suppose that the mesh spacing is small enough that the region $\overline{PAFB}$ has almost uniform strain and stress throughout. The sides $\overline{AP}$ and $\overline{PB}$ will be straight to a good approximation. Then (at least in the infinitesimal case) the sides have uniform stress distributions acting on them and can be throught of as rigid (because they are straight and therefore cannot bend). Take side $\overline{PB}$

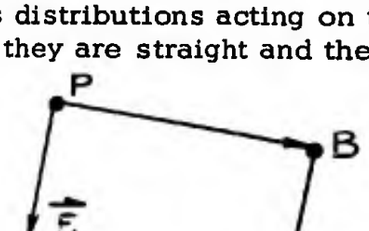

The stress distribution $\vec{S}$ can be replaced by two forces $\vec{F}_1$ and $\vec{F}_2$, which are equivalent to $\vec{S}$. If the side is rigid, force $\vec{F}_1$ equals $\vec{F}_2$. It seems then, that the force on P due to the stress distribution on $\overline{PB}$ is $\vec{F}_1$. $\vec{F}_1$ is given by

$$\vec{F}_1 = \vec{F}_2 = 1/2\ \vec{S} * (\text{length of } \overline{PB})$$

where $\vec{S}$ is the stress vector across $\overline{PB}$. The side $\overline{PA}$ is treated similarly. Then the effects of other quadrants are added to form the net resultant force $\vec{F}$, acting on P.

Note that $\vec{F}_2$ appears to contribute a moment around point P that has not been taken into account. Even though $\vec{F}_2$ does, in effect, produce a moment around P, it is accounted for when the resultant at point B is calculated and does not <u>directly</u> enter into the resultant at P. Otherwise the effect of $\vec{F}_2$ would be counted more than once, i.e., once at point P, and again at point B.

If P has mass m, then Newton's law is

$$\vec{F} = m\vec{a}$$

To avoid problems equivalent to covariant differentiation, the stress vectors across the sides of the quadrants are expressed in the underlying spatial coordinates and then added to form the resultant. This is easy because the side vectors are known in the underlying coordinates anyway.

It should be shown more clearly that the above formulation is at least approximately equivalent to the accepted tensor form of Newton's law.

Let us apply Newton's law to a very small material volume

element. Note that the mass in a chosen material element is always constant, but the density may vary. Newton's law gives

$$\frac{d}{dt} \int^{V} \rho \, \vec{v} \, dV = \int^{S} \vec{T} \, dA$$

where V is the volume

ρ is the density

$\vec{v}$ is the velocity vector

S is the surface

dA is the surface element

$\vec{T}$ is the stress vector across the surface.

Now the following approximation is reasonable if the volume element is small enough: The mass is assumed to be located at a point in the middle of the volume. Equivalently, the volume may be chosen around the mass point P.

Then $$\frac{d}{dt} \int^{V} \rho \vec{v} \, dV$$

becomes $$m \frac{d\vec{v}}{dt}$$

where m is the mass in the volume.

Remember that m remains constant because we have taken a material volume element.

The surface integral of the stress is simplified because the total surface is composed of several coordinate surfaces. The integral over the i-th face of the element is

$$\int^{\text{side i}} \frac{t^{ji}}{\sqrt{g^{ii}}} \vec{g}_i \, dA_{\text{side i}}$$

the equation of motion in the discrete variable model becomes

$$m \frac{d\vec{v}}{dt} = \sum_{\text{sides}}^{\text{all}} \int^{\text{side i}} \frac{t^{ji}}{\sqrt{g^{ii}}} \vec{g}_i \, dA \text{ side i}$$

$$m \frac{dv}{dt} = \sum_{\text{sides}}^{\text{all}} \frac{t^{ji}}{\sqrt{g^{ii}}} \hat{g}_i A_{\text{side } i}$$

where A side i is the area of side i.

Since the stress and strain are assumed to be almost constant throughout a given quadrant, this equation of motion is equivalent to the one derived previously in a more intuitive fashion. This is because the integral taken over the surface is identical to the integral taken on the sides determined by the basis vectors.

$\overline{PACB}$ is a parallelogram and the stress and strain are assumed to be uniform throughout its area. The integral of the stress vector along $\overline{CB}$ must therefore be the same as the integral along $\overline{PA}$.

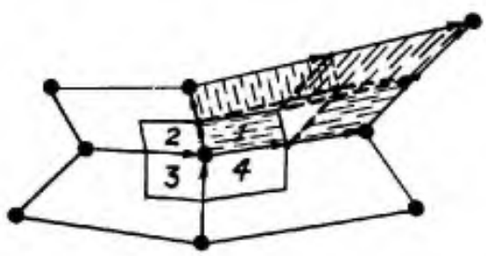

The vectors determining the volumes are 1/2 the basis vectors so that the same volume will not be counted more than once. The dotted lines show a few of the parallelepipeds formed by assuming that each two adjacent basis vectors determine a local metric.

The regions labeled 1, 2, 3 and 4 are comprising the volume associated with point P. Similar volumes are defined for all the other points. This seems to be an approximation which is reasonable until the deformation becomes very severe.

3.5 A Three-Dimensional Mesh With Cylindrical Symmetry

The assumption of cylindrical symmetry throughout the deformation results in considerable simplification of the formulae.

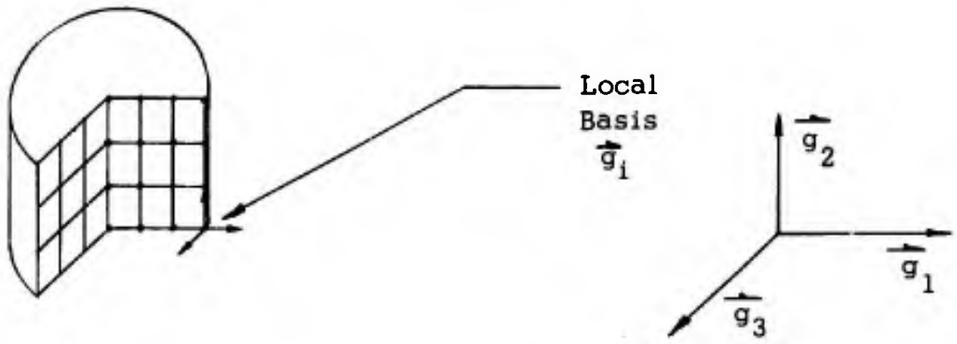

Since cylindrical symmetry is retained, the metric must always be of the form

$$g_{ij} = \begin{bmatrix} g_{11} & g_{12} & 0 \\ g_{21} & g_{22} & 0 \\ 0 & 0 & r^2 \end{bmatrix}$$

where $r = y^1$ is the spatial distance from the axis to the material point in question.

The initial metric is of the form

$$G_{ij} = \begin{bmatrix} 1 & 0 & 0 \\ 0 & 1 & 0 \\ 0 & 0 & r_o^2 \end{bmatrix}$$

where r_o is the distance from the axis at time zero.

Thus the strain tensor is

$$e_{ij} = 1/2 \begin{bmatrix} g_{11}-1 & g_{12} & 0 \\ g_{21} & g_{22-1} & 0 \\ 0 & 0 & r^2-r_o^2 \end{bmatrix}$$

Suppose we are using the following stress-strain relation:

$$t_i^j = a\, g_i^j\, e_k^k + b e_i^j + C\dot{D}_i^j$$

where a, b and c are any zero order tensors.

Clearly the stress tensor will be of the form

$$t_i^{\ j} = \begin{bmatrix} t_1^{\ 1} & t_1^{\ 2} & 0 \\ t_2^{\ 1} & t_2^{\ 2} & 0_3 \\ 0 & 0 & t_3^{\ 3} \end{bmatrix}$$

and

$$t^{ij} = \begin{bmatrix} t^{11} & t^{12} & 0 \\ t^{21} & t^{22} & 0 \\ 0 & 0 & t^{33} \end{bmatrix}$$

Probably the simplest way to derive the so-called "hoop stress" that must be added to the case of a semi-infinite slab, is to look at a cylindrical volume element geometrically.

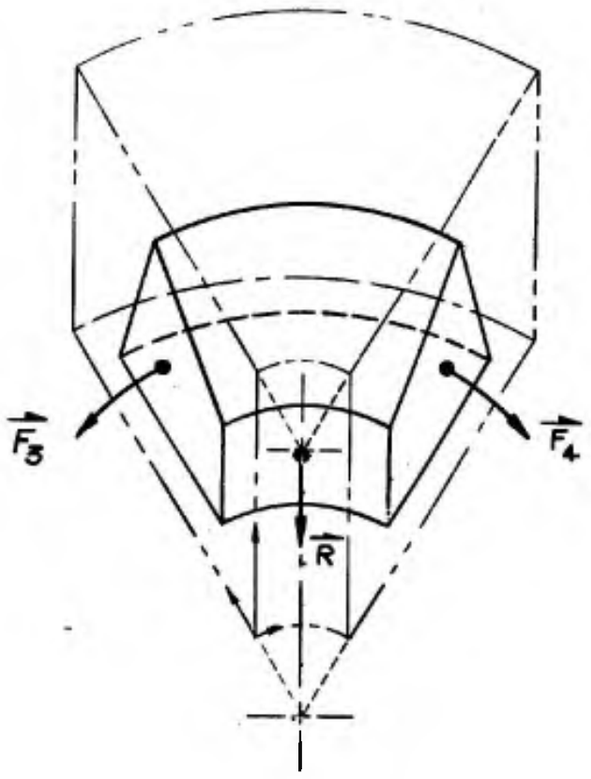

The forces $\vec{F}_3$ and $\vec{F}_4$ are equal in magnitude as a result of the symmetry. However, they are not in the same direction, and when they are added their resultant will be in the $\vec{R}$ direction.

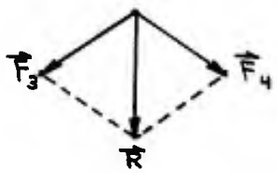

This exaggerated figure shows the resultant hoop stress $\vec{R}$.

4. COMPUTATIONS

4.1 Refinement of the Difference Approximation in the Time Dimension

The time derivatives involved in the discrete variable model must be approximated in some way using values at discrete time points. The first approximation we used was based on the assumption that the force during an interval of time was constant and was the ending value. This was too crude an assumption as we found out later.

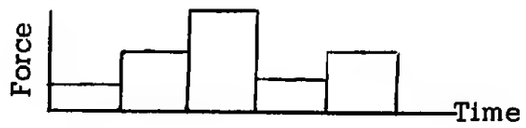

Due to the dissymmetry of this force rule, the computations introduced energy into the system as the forces at material points increased and then decreased (as the elastic waves traveled past).

A way to remedy this error is to use a symmetrical force rule. The generating assumption will be that the force changes linearly with time during a time interval.

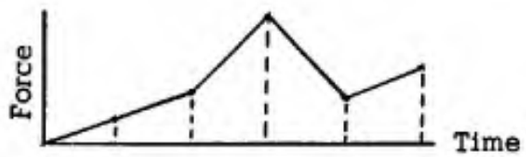

This eliminates erroneous gain or loss of energy because the material now loads and unloads symmetrically.

The details are presented in the following section.

4.2 Kinematics for a Linear Change of Force Within a Time Interval

The results are derived in only one spatial dimension for simplicity. Since we are using spatial coordinates which are orthonormal, this easily extends to more dimensions.

Suppose that during a time interval $\Delta t_n = t_n - t_{n-1}$, the force F is given by

$$F = F_{n-1} + \left[\frac{F_n - F_{n-1}}{\Delta t_n}\right](t - t_{n-1})$$

$$F = F_{n-1} + \frac{\Delta F_n}{\Delta t_n} (t - t_{n-1})$$

where $\Delta F_n = F_n - F_{n-1}$

Graphically

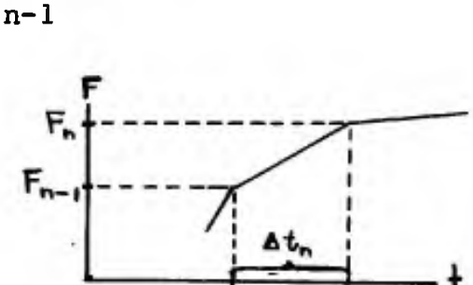

During time interval n, there will be a change in velocity due to an accelerational force F

$$\frac{dV}{dt} = \frac{1}{m} F$$

or equivalently $$\Delta V_n = \frac{1}{m} \int_{t_{n-1}}^{t_n} F \, dt$$

To simplify the calculus we make a change of variable: $t_{old} = t_{new} + t_{n-1}$. Then the velocity during the interval is

$$V = V_{n-1} + \frac{1}{m} \int_0^t F \, dt$$

The change in position Δx is

$$\Delta x_n = \int_0^{\Delta t_n} \left[V_{n-1} + \frac{1}{m} \int_0^t F \, dt \right] dt$$

$$\Delta x_n = V_{n-1} \, \Delta t_n + \frac{1}{m} \int_0^{\Delta t_n} \int_0^t F \, dt \, dt$$

At the end of time interval n

$$x = x_n = x_{n-1} + \Delta x_n$$

and $$V = V_n = V_{n-1} + \Delta V_n$$

The integral $\int_0^{\Delta t_n} F\,dt$ becomes

$$\int_0^{\Delta t_n} F\,dt = \left[F_{n-1}\, t + \frac{\Delta F_n}{\Delta t_n}\, \frac{t^2}{2} \right]_0^{\Delta t_n}$$

so that

$$m\ \Delta V_n = F_{n-1}\ \Delta t_n + \frac{\Delta F_n}{\Delta t_n}\ \frac{\Delta t_n^{\,2}}{2}$$

$$m\ \Delta V_n = F_{n-1}\ \Delta t_n + \frac{\Delta F_n\ \Delta t}{2}$$

The second integral becomes

$$\int_0^{\Delta t_n} \int_0^{t} F\,dt\,dt = \int_0^{\Delta t_n} \left[F_{n-1}\, t + \frac{\Delta F_n}{\Delta t_n}\, \frac{t^2}{2} \right] dt$$

$$= \left[\frac{F_{n-1}\, t^2}{2} + \frac{\Delta F_n}{\Delta t_n}\, \frac{t^3}{6} \right]_0^{\Delta t_n}$$

$$= \frac{F_{n-1}\ \Delta t_n^{\,2}}{2} + \frac{\Delta F_n\ \Delta t_n^{\,2}}{6}$$

$$= \left[\frac{3\, F_{n-1} + \Delta F_n}{6} \right] \Delta t_n^{\,2}$$

Substituting and simplifying, we get more explicit expressions for the quantities V_n, Δx_n, x_n, and acceleration, a_n.

<u>Velocity</u> (at the end of interval n)

$$V_n = V_{n-1} + \frac{1}{m} \int_0^{\Delta t_n} F\,dt$$

$$V_n = V_{n-1} + \frac{1}{m} \left[F_{n-1} + \frac{\Delta F_n}{2} \right] \Delta t$$

Change in Position (during the interval n)

$$\Delta x_n = V_{n-1} \quad \Delta t_n + \frac{1}{m} \int_o^{\Delta t_n} \int_o^t F \, dt \, dt$$

$$\Delta x_n = V_{n-1} \quad \Delta t_n + \frac{1}{m} \left[\frac{3F_{n-1} + \Delta F_n}{6} \right] \Delta t_n^2$$

$$\Delta x_n = V_{n-1} \quad \Delta t_n + \frac{\Delta t_n^2}{6m} \left[2 F_{n-1} + F_n \right]$$

Position (at end of interval n)

$$x_n = x_{n-1} + \Delta x_n$$

Acceleration (at end of interval n)

$$a_n = \frac{F_n}{m}$$

From the expression for Δx_n we find F_n

$$3 F_{n-1} + \Delta F_n = \frac{6m}{\Delta t_n^2} \left[\Delta x_n - V_{n-1} \quad \Delta t_n \right]$$

$$F_n + 2 F_{n-1} =$$

$$F_n = \frac{6m}{\Delta t^2} \left[\Delta x_n - V_{n-1} \quad \Delta t_n \right] - 2 F_{n-1}$$

So that the acceleration is

$$a_n = \frac{6}{\Delta t_n^2} \left[\Delta x_n - V_{n-1} \quad \Delta t_n \right] - 2/m \, F_{n-1}$$

Kinetic Energy (at the end of interval n)

$$\overline{KE}_n = \frac{1}{2} \, m \, V_n^2$$

using the expression for V_n

$$\overline{KE}_n = \frac{1}{2} m \left[V_{n-1} + \frac{1}{m} \left(F_{n-1} + \frac{\Delta F_n}{2} \quad \Delta t \right] \right]^2$$

Change in Total Work (during the interval n)

$$\Delta W_n = \int_0^{\Delta t_n} F \frac{dx}{dt} dt$$

The expression for the force is

$$F = F_{n-1} + \frac{\Delta F_n}{\Delta t_n} t$$

The differential dx must be expressed in terms of the differential dt. We express x as a function of time (during interval n) and differentiate with respect to time t.

$$x = x_{n-1} + \left[V_{n-1} t + \frac{1}{m} \int_0^t \int_0^t F \, dt \, dt \right]$$

$$\frac{dx}{dt} = V_{n-1} + \frac{1}{m} \int_0^t F \, dt$$

Substituting the expression for F

$$\frac{dx}{dt} = V_{n-1} + \frac{1}{m} \int_0^t \left[F_{n-1} + \frac{\Delta F_n}{\Delta t_n} t \right] dt$$

$$\frac{dx}{dt} = V_{n-1} + \frac{1}{m} F_{n-1} t + \frac{1}{2m} \frac{\Delta F_n}{\Delta t_n} t^2$$

Substituting this in the expression for ΔW_n we get

$$\Delta W_n = \int_0^{\Delta t_n} F \frac{dx}{dt} dt$$

$$\Delta W_n = \int_0^{\Delta t_n} \left[F_{n-1} + \frac{\Delta F_n}{\Delta t_n} t \right] \left[V_{n-1} + \frac{1}{m} F_{n-1} t + \frac{1}{2m} \frac{\Delta F_n}{\Delta t_n} t^2 \right] dt$$

$$\Delta W_n = \int_0^{\Delta t_n} \left(F_{n-1} V_{n-1} \right) + \left[\frac{1}{m} \left(F_{n-1} \right)^2 + \frac{\Delta F_n}{\Delta t_n} V_{n-1} \right] t$$

$$+ \left[\frac{1}{m} \frac{\Delta F_n}{\Delta t_n} F_{r-1} + \frac{1}{2m} \frac{\Delta F_n}{\Delta t_n} F_{n-1}\right] t^2$$

$$+ \frac{1}{2m}\left(\frac{\Delta F_n}{\Delta t_n}\right) t^3 \, dt$$

$$\Delta W_n = V_{n-1} F_{n-1} \Delta t + \frac{1}{2} V_{n-1} \Delta F_n \Delta t_n + \frac{1}{2m} \left(F_{n-1} \Delta t\right)^2$$

$$+ \frac{1}{3m} \Delta F_n F_{n-1} \Delta t^2 + \frac{1}{6m} F_{n-1} \Delta F_{n-1} \Delta t^2$$

$$+ \frac{1}{8m} \Delta F_n^2 \Delta t^2$$

5. REFERENCES FOR THEORY AND COMPUTATIONAL METHODS

1. Eringen, A. Cemal, "Nonlinear Theory of Continuous Media," McGraw-Hill Book Company, Inc., New York (1962).

2. Sokolnikoff, I. S., "Tensor Analysis," New York (1951).

3. Sokolnikoff, I. S., "Mathematical Theory of Elasticity," McGraw-Hill Book Company, Inc., New York (1956).

4. Houwink, R., "Elasticity, Plasticity and Structure of Matter," Dover Publications, Inc., New York (1958).

5. Lichnerowicz, A., "Elements of Tensor Calculus," John Wiley & Sons, Inc., New York (1963).

6. Wrede, Robert C., "Vector and Tensor Analysis," John Wiley & Sons, Inc., New York (1963).

7. Hodgman, Charles D., "Handbook of Chemistry and Physics," Chemical Rubber Publishing Co., Cleveland, Ohio (1940).

8. Riney, T. D., "Theoretical Hypervelocity Impact Calculations Using the Picwick Code," Air Proving Ground Center, Eglin Air Force Base, Florida (1963).

9. Wylie, C. R., Jr., "Advanced Engineering Mathematics," McGraw-Hill Book Company, Inc., New York (1960).

10. Ralston, Anthony and Herbert S. Wilf, "Mathematical Methods for Digital Computers," John Wiley & Sons, Inc., New York (1962).

11. Coulson, C. A., "Waves," Interscience Publishers, Inc., New York (1962).

12. Thomas, Tracy Y., "Plastic Flow and Fracture in Solids," Academic Press, New York (1961).

13. Grinter, L. E., "Numerical Methods of Analysis in Engineering," MacMillan Company, New York (1949).

14. Hildebrand, F. B., "Introduction to Numerical Analysis," McGraw-Hill Book Company, Inc. (1956).

15. Webster, A. G., "Partial Differential Equations of Mathematical Physics," Dover Publications, Inc. (1955).

16. Thomas, Tracy Y., "Tensor Analysis and Differential Geometry," Academic Press, New York (1961).

17. Lapidus, Leon, "Digital Computation for Chemical Engineers," McGraw-Hill Book Company, Inc., New York (1962).

18. Freudenstein, Ferdinand and Bernard Roth, "Numerical Solution of Systems of Nonlinear Equations," Journal of the Association for Computing Machinery, Assoc. for Computing Machinery, (1963).

19. Brode, H. L. and R. L. Bjork, "Cratering From a Megaton Surface Burst," Proceedings of the Geophysical Laboratory, Lawrence Ratiation Laboratory Cratering Symposium, Livermore, Calif. (1961).

20. Rajnak, S. and F. Hauser, "Plastic Wave Propagation in Rods," Symposium on Dynamic Behavior of Materials, ASTM Special Technical Publications No. 336, American Soc. for Testing and Materials, Philadelphia, Pa. (1962).

21. Harlow, Francis H., "Two-Dimensional Hydrodynamic Calculations," Los Alamos Scientific Laboratory, Mex. (1959).

22. Wilkins, Mark L. and Richard Giroux, "The Calculation of Stress Waves in Solids," Proceedings of the Sixth Symposium on Hypervelocity Impact (1963).

23. Kolsky, H., "Stress Waves in Solids," Dover Publications, Inc., New York (1963).

24. Daly, Bart J., "The Bounding of Instabilities of the PIC Difference Equations, Los Alamos Scientific Laboratory, Mex. (1962).

25. Korn, Granino A., "Mathematical Handbook for Scientists and Engineers," McGraw-Hill Book Company, New York (1961).

26. Pearson, Carl E., "Theoretical Elasticity," Harvard University Press, Cambridge, Mass. (1959).

27. Jacobsen, Lydik S., and Ayre, Robert S., "Engineering Vibrations," McGraw-Hill Book Company, New York (1958).

28. Shaw, F. S., "Relaxation Methods," Dover Publications (1953).

29. Synge, J. L., and Schild, A., "Tensor Calculus," University of Toronto Press, Toronto (1961).

30. Thomas, Tracy Y., "Plastic Flow and Fracture in Solids," Academic Press, New York (1961).

31. Bellman, Richard, "Introduction to Matrix Analysis," McGraw-Hill Book Company, New York, (1960).

32. Birkhoff, Garrett and MacLane, Saunders, "A Survey of Modern Algebra," Revised Ed., MacMillan Co., New York (1962).

33. Condon, E. U. and Odishaw, H. editors, "Handbook of Physics," McGraw-Hill Book Co., New York (1958).

34. Novozhilov, V. V., "Foundations of the Nonlinear Theory of Elasticity," Graylock Press, Rochester, N.Y. (1953).

35. Murnaghan, Francis D., "Introduction to Applied Mathematics," Dover Publications, New York (1963).

36. Shanley, F. R., "Strength of Materials," McGraw-Hill Book Co., New York (1957).

37. Coulson, C. A., "Waves," Interscience Publishers, Inc., New York (1961).

38. Beckenbach, Edwin F., editor, "Modern Mathematics for the Engineer," McGraw-Hill Book Co., New York (1956).

39. Coburn, Nathaniel, "Vector and Tensor Analysis," MacMillan Co., New York (1955).

40. Utah Research and Development Co., "Theoretical and Experimental Study of Low-Velocity Penetration Phenomena - Final Report, Phases I and II," Contract DA 19-129-AMC-150(X), (1964).

6. MEASUREMENT OF DEFORMATION

An experimental program was started for the purposes of obtaining data for guiding and checking theoretical work and to serve as an independent approach to a solution of the penetration problem.

Equipment has been developed for shooting balls against stretched wires and observing the transient deformation. The results are to supply one-dimensional material-property data for the computer program. Impacts into plates or for rods into rods can also be observed to obtain data for two-dimensional properties. The techniques and equipment will be briefly discussed and the results illustrated.

High-Speed-Impact Photography

Much work has been done by other investigators to develop photographic techniques for studies of impact phenomena. The most successful photographs result when shadowgraphs can be used. Less success has been obtained with front-lighting, or reflected-light methods. Some of the data desired in this project deal with material deformation and movement. To make these data quantitative, it is necessary to determine the position of the material as a function of time. As this is difficult to do with shadowgraphs of opaque materials, various front-lighting techniques were investigated. Back lighting of transparent or translucent materials can be useful when opaque reference marks are placed on the material surface. These marks are outlined by light passing through the material. With equipment now in use, six photographs can be taken at any specified time during impact. Figure 1 is a sketch showing the arrangement of the equipment.

Gun

The gun is smooth bored and chambered for 50-caliber cartridges. One-half inch diameter balls and rods have been accelerated with it. Velocities up to about 6,600 ft/sec (2 km/sec) can be obtained using gunpowder as the propellant. A special attachment permits the use of pressurized air for shooting at very low velocities.

Velocity Measurements

The projectile velocity is determined for each shot by measuring the time of flight between two probes. As the projectile passes each probe, a circuit is completed and a pulse goes to the oscilloscope.

Camera

The camera is an Electro Optical Instrument Company, Kerr Cell framing camera, Model KFC-600/B. With the particular delay generators

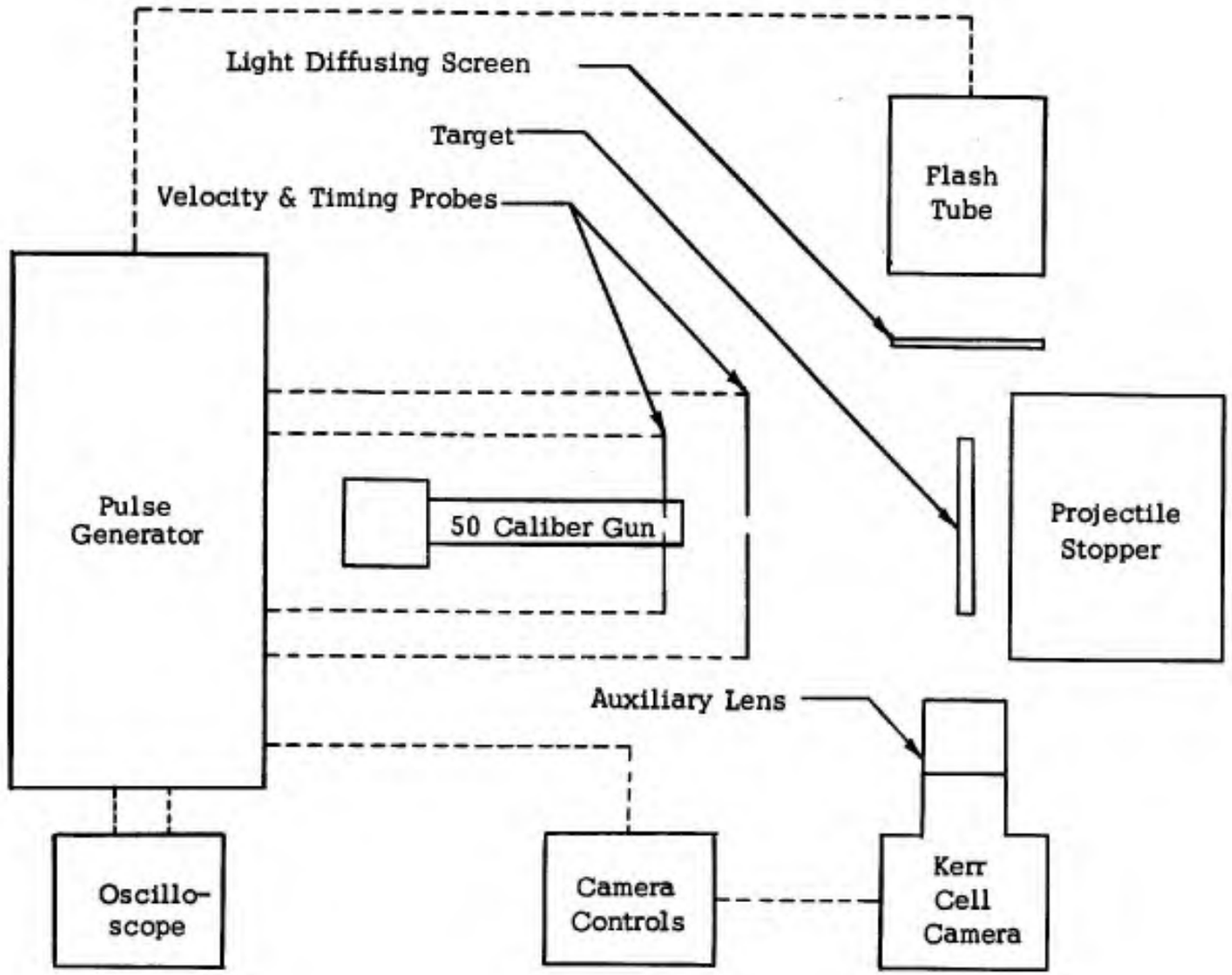

FIGURE 1. Diagram Showing the Positioning of Equipment Used in Taking Photographs of Impact Events.

used, a series of six pictures can be obtained at intervals of from 0 to 50 μ sec. The exposure time of each shutter is 0.2 μ sec. As shown in Figure 1, the camera is triggered by the pulse from the second probe. Both shadowgraphs and reflected-light photographs can be obtained by changing the position of the flash tube. With the position shown in Figure 1, shadowgraphs are obtained. An auxiliary lens is placed in front of the camera lens to increase the size of the target image at the film plane.

Flash Tube

The flash tube is a General Electric, Model FT-503. At 4000 volts it has a maximum output of 3200 watt-seconds. The pulse width at half maximum intensity is about 100 microseconds. To get good reflected-light photographs, it is necessary to synchronize the operation of the camera and flash tube so that the photographs are taken when the light output is at a maximum.

Shadowgraphs

Figures 2, 3 and 4 are shadowgraphs taken with the equipment arranged as shown in Figure 1. The grid lines shown are 1 cm apart and are about 3 inches behind the target. The targets in Figures 2 and 3 are 1/4" square plexiglass rods. They are shown in vertical position in the pictures. Reference lines are drawn on the front surfaces with black ink. Light passing through the plexiglass reveals these lines. The numbers below the pictures indicate time in microseconds after the shorting of the second probe. The velocity of the projectile in Figure 2 is 361 ft/sec (0.11 km/sec). In Figure 3 it is about 2,300 ft/sec (0.7 km/sec). Qualitative differences in the amount of damage caused at the different velocities are readily apparent. At the low velocity, fracturing occurs at some distance from the point of impact; while at the high velocity, the damage is more localized. Figure 4 shows impact against a 0.1" copper wire at a velocity of 1,960 ft/sec (0.6 km/sec).

Reflected-Light Photographs

To take reflected-light photographs, the arrangement of equipment shown in Figure 1 is changed so that the front surface of the target is illuminated. Ordinary metal surfaces do not reflect enough light to reveal details. To overcome this difficulty, surfaces are painted with flat white paint. Some examples are shown in Figure 5. In (a) a narrow strip of paper is impacted by a steel ball; in (b), impact occurs against a 0.028" diameter steel piano wire; and in (c) a 0.1" diameter copper wire is shown shortly before impact. In (c), alternate sections of the wire are painted to give a dashed effect and make possible the identification of a particular point from one frame to another.

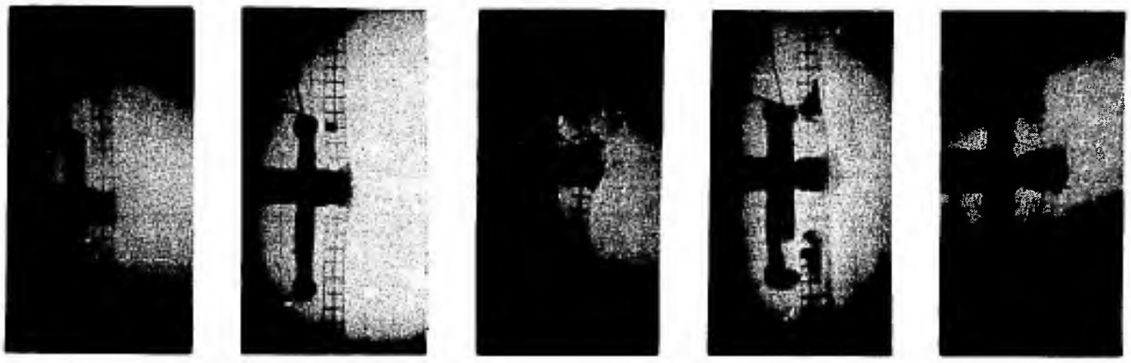

50 80 120 140 160

FIGURE 2. Shadowgraphs Showing the Impact of a 1/2-inch Diameter Steel Ball Against a 1/4-inch Square Plexiglass Rod at a Velocity of 0.11 km/sec. The Numbers Indicate Time (in μsec) After Triggering of the Camera.

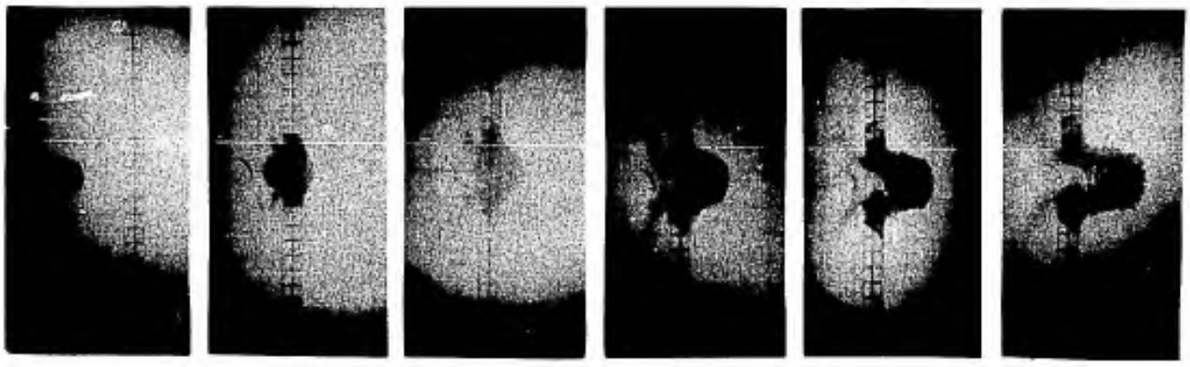

50 90 100 110 120 130

FIGURE 3. Shadowgraphs Showing the Impact of a 1/2-inch Diameter Steel Ball Against a 1/4-inch Square Plexiglass Rod at a Velocity of About 0.7 km/sec. The Numbers Indicate Time (in μsec) After Triggering of the Camera.

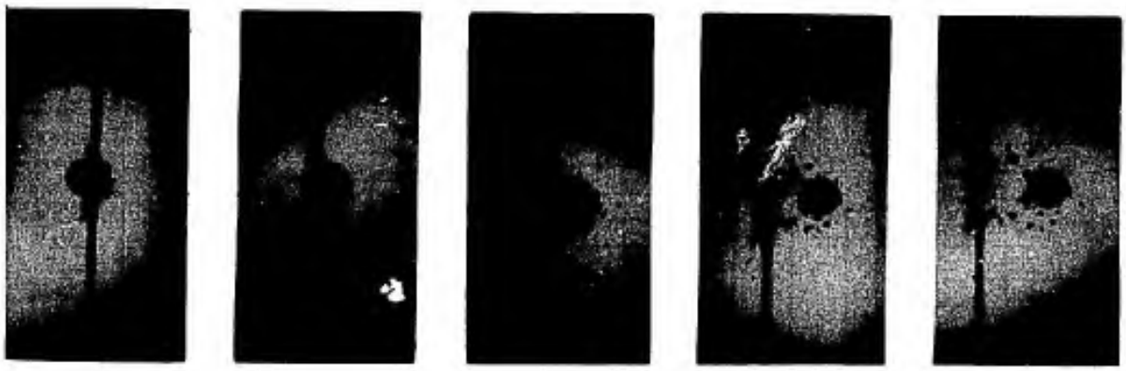

58 66 74 82 90

FIGURE 4. Shadowgraphs Showing the Impact of a 1/2-inch Diameter Steel Ball Against a 0.1-inch Diameter Copper Wire at a Velocity of 0.6 km/sec. The Numbers Indicate Time (in μsec) After Triggering of the Camera.

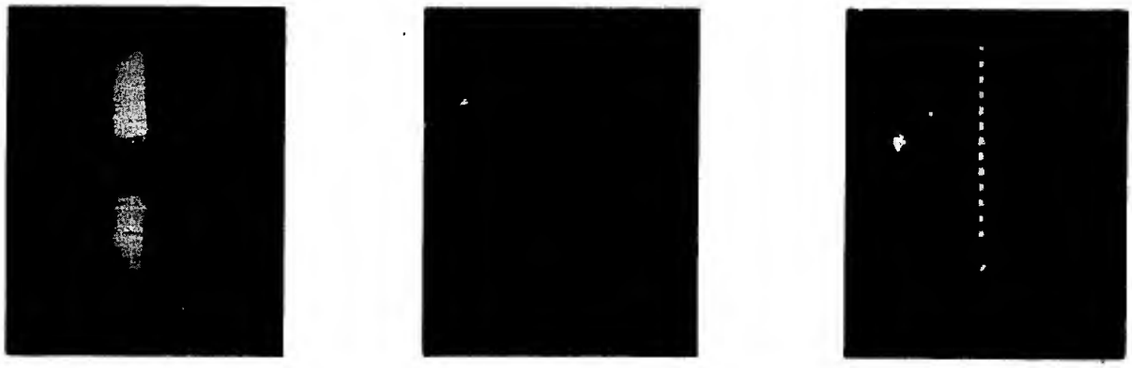

(a) (b) (c)

FIGURE 5. Reflected-light Photographs: (a) A Narrow Strip of Paper Impacted on its Edge by a 1/2-inch Diameter Steel Ball, (b) A 0.028-inch Diameter Steel Piano Wire Impacted by a 1/2-inch Diameter Steel Ball, (c) A 0.1-inch Diameter Copper Wire Shortly Before Impact. In All Cases the Surfaces of the Targets were Covered with Flat White Paint.

The square grids shown in Figure 5 were formed by double exposure of the film. In the first exposure, a plastic plate with the grid pattern scribed on it was placed in the target position and photographed. For the second exposure, the plastic plate was removed, the target was then positioned and the shot made and photographed. This procedure was developed so that a well defined and accurately spaced grid would appear in each frame to help in making measurements of target deformation and movement.

7. ENERGY OF DEFORMATION

The amount of energy used in deforming target material is of particular interest in penetration problems. This is so because such information is important in guiding and checking impact theories as well as providing engineering data.

Some work has been done[1] concerning this problem in which low-velocity impacts involving identical rods of lead, copper, and steel were observed. The fraction of the kinetic energy of the projectile going into internal energy in projectile and target was calculated for each shot by knowing the impact velocity of the projectile rod and the knock-on velocity of the target rod. The deformed rods used in these studies have been made available. From them, specimens representing a wide impact velocity range have been selected and the total amount of deformation in each one has been determined. In determining total deformation, the degree of deformation (which is defined as the fractional change in the area of a plane section through the rod perpendicular to the axis of the rod), was determined for each of several sections in each rod. This is shown by the equation:

$$d = \frac{A - A_o}{A_o} = \frac{A}{A_o} - 1$$

where d = degree of deformation

A_o = area of section before deformation

A = area of section after deformation.

Material is said to have undergone unit deformation when $d = 1$.

Total deformation was calculated by multiplying the degree of deformation of each section of the rod by its volume and then getting the sum of these products for all sections considered. This procedure is described by the equation:

$$D_T = \sum_i d_i V_i$$

where D_T = total deformation in the rod

d_i = the degree of deformation in each section considered

V_i = the volume of each section.

In the measurements and calculations described above, it was

assumed that a plane which was perpendicular to the rod axis before impact remained a plane during the deformation process. It was also assumed that the degree of deformation was uniform at all points on a particular plane.

Values were computed for the amount of energy necessary to produce unit deformation in one cubic centimeter of material. This is defined as energy per unit of deformation. These values are shown plotted in Figure 6 as a function of projectile impact velocity. As would be expected, the values are greatest for steel and least for lead. It is of interest that the values for copper and steel decrease as the impact velocity increases. This indicates that the deformation mechanism is more efficient at higher velocities.

The straight lines describing the data points are shown extrapolated to zero velocity. It is found that the deformation energy values at that point are approximately proportional to the static shear strengths of the metals. It would be of interest to determine deformation energy values under static conditions and compare them with those indicated by the extrapolated lines in Figure 6.

It appears doubtful that these energy measurements can be made successfully with nonductile materials. The possibility of doing it and of photographing the deformation will be examined next quarter.

---

[1]Technical Report UU-14, Final Report on Contract AF 04(694)-259, High Velocity Laboratory, University of Utah, Parts I and II (1964).

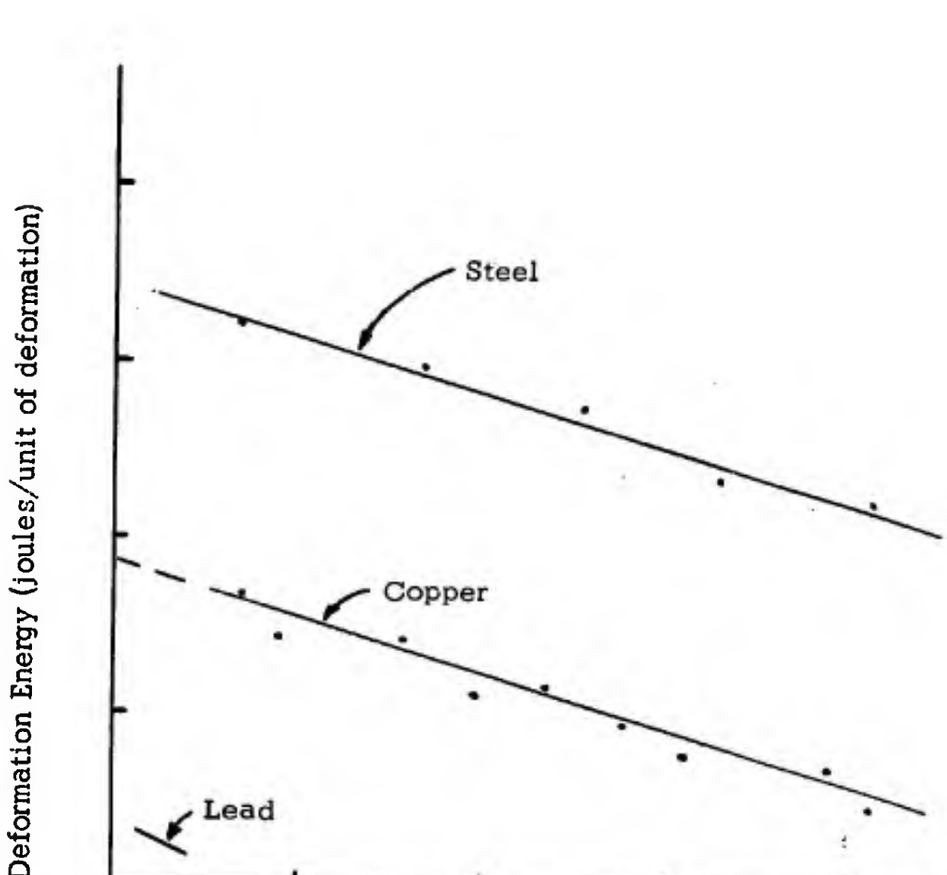

FIGURE 6. Energy Per Unit of Deformation Shown Plotted as a Function of Projectile Impact Velocity For Rod-To-Rod Impact.